JCI insight

RESEARCH ARTICLE

Dual inhibition of complement factor 5 and leukotriene B_4 synergistically suppresses murine pemphigoid disease

Tanya Sezin,[1] Sripriya Murthy,[1] Claudia Attah,[1] Malte Seutter,[1] Maike M. Holtsche,[1] Christoph M. Hammers,[1] Enno Schmidt,[2,3] Fibi Meshrkey,[1] Sadegh Mousavi,[1] Detlef Zillikens,[1,3] Miles A. Nunn,[4] and Christian D. Sadik[1,3]

[1]Department of Dermatology, Allergy, and Venereology, [2]Lübeck Institute for Experimental Dermatology, and [3]Center for Research on Inflammation of the Skin, University of Lübeck, Lübeck, Germany. [4]Akari Therapeutics, London, United Kingdom.

The treatment of most autoimmune diseases still relies on systemic immunosuppression and is associated with severe side effects. The development of drugs that more specifically abrogate pathogenic pathways is therefore most desirable. In nature, such specificity is exemplified, e.g., by the soft tick–derived biotherapeutic Coversin, which locally suppresses immune responses by inhibiting complement factor 5 (C5) and leukotriene B_4 (LTB_4). C5a, a proteolytic fragment of C5, and LTB_4 are critical drivers of skin inflammation in pemphigoid diseases (PDs), a group of autoimmune blistering skin diseases. Here, we demonstrate that both Coversin and its mutated form L-Coversin, which inhibits LTB_4 only, dose dependently attenuate disease in a model of bullous pemphigoid–like epidermolysis bullosa acquisita (BP-like EBA). Coversin, however, reduces disease more effectively than L-Coversin, indicating that inhibition of C5 and LTB_4 synergize in their suppressing effects in this model. Further supporting the therapeutic potential of Coversin in humans, we found that C5a and LTB_4 are both present in the blister fluid of patients with BP in quantities inducing the recruitment of granulocytes and that the number of cells expressing their receptors, C5aR1 and BLT1, respectively, is increased in perilesional skin. Collectively, our results highlight Coversin and possibly L-Coversin as potential therapeutics for PDs.

Introduction

Pemphigoid diseases (PDs) are a group of chronic autoimmune blistering skin diseases featuring an autoantibody-driven immune response against different proteins of the dermal-epidermal adhesion complex (1). Upon autoantibody deposition at the dermal-epidermal junction (DEJ), neutrophils and eosinophils are recruited to the DEJ, which is essential for the formation of inflammatory skin lesions, including blisters and erosions (1). PDs are associated with an increase in mortality. Bullous pemphigoid (BP), for example, is associated with a 3.6-fold increase in mortality in the first year after diagnosis (2, 3). The cause for the increased mortality is poorly understood, but adverse effects of immunosuppressants, in particular steroids, are believed to contribute substantially (2), illustrating the need for more selective therapeutic agents associated with fewer side effects.

Selectively disrupting the recruitment of granulocytes into the skin or their activities within the skin may be key to treating PDs. Using the antibody transfer mouse models of BP-like epidermolysis bullosa acquisita (EBA) and of BP, we previously discovered that the chemoattractant/chemoreceptor pairs leukotriene B_4/BLT1 (LTB_4/BLT1) and activated complement fragment C5a/C5aR1 are critical for the recruitment of neutrophils into the skin and, consequently, for skin inflammation (4–8). In support of roles for LTB_4/BLT1 and C5a/C5aR1 in PDs, LTB_4 and the C5a precursor complement factor 5 (C5) have been shown to be present in blister fluid and perilesional skin, respectively, of patients with BP (9–11). Hence, LTB_4/BLT1 and C5a/C5aR1 are potential therapeutic targets in BP and other PDs.

Ornithodoros moubata complement inhibitor (OmCI), a lipocalin present in the saliva of this blood-sucking tick, has evolved both to inhibit C5 activation and to capture LTB_4 (12). OmCI binds tightly to human and murine C5, thus preventing its proteolysis to C5a and C5b through C5 convertase activity, and sequesters LTB_4 with high binding affinity (13–16). Notably, the binding of C5 and LTB_4 to OmCI have no

Conflict of interest: MAN is an employee of Akari Therapeutics, which currently develops Coversin as novel therapeutic. MAN and CDS are both listed as inventors on a patent application for the use of Coversin in bullous pemphigoid (patent application number 1706404.9, United Kingdom).

Submitted: March 4, 2019
Accepted: July 9, 2019
Published: August 8, 2019.

Reference information: *JCI Insight*. 2019;4(15):e128239. https://doi.org/10.1172/jci.insight.128239.

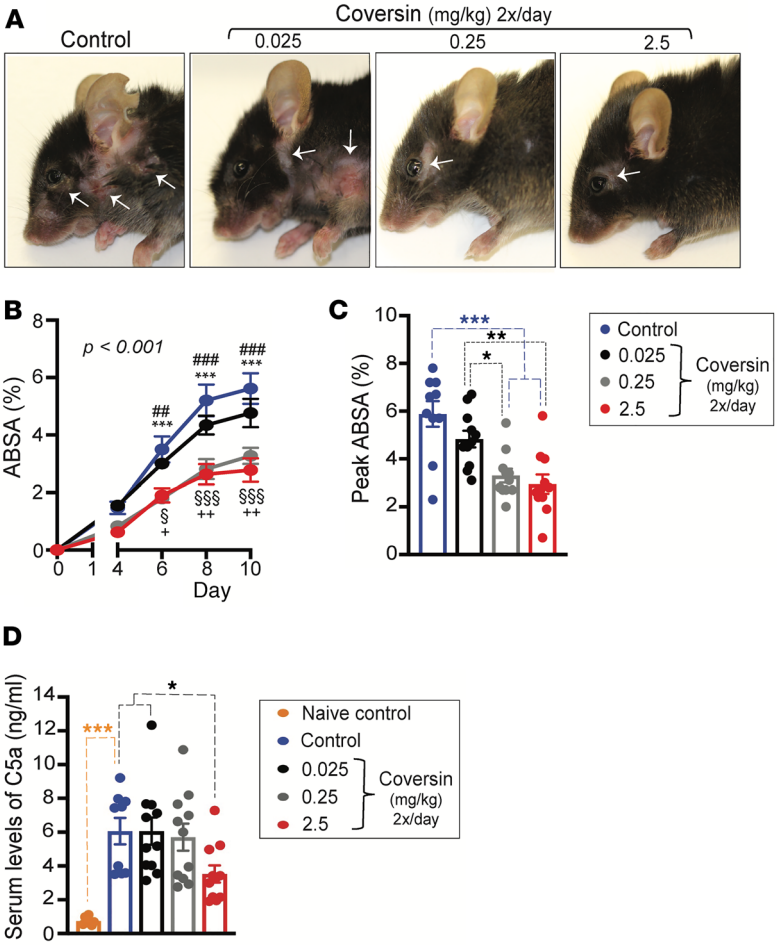

Figure 1. Coversin dose dependently suppresses skin inflammation in a preventative setting. Effect of varying doses of Coversin administered twice daily starting 4 days before the first application of anti-COL7c IgG. (**A**) Representative clinical presentation at the end of the experiment on day 10. White arrows indicate BP-like EBA skin lesions. (**B**) Progression of disease benchmarked as percentage of the total body surface area affected by skin lesions (ABSA). Results were pooled from 2 independent experiments and are presented as mean ± SEM (n = 10–11 mice per group). Data were analyzed using 2-way ANOVA with Holm-Šídák's multiple-comparisons test. ##P < 0.01, and ###P < 0.001 compared with 2.5 mg/kg body weight Coversin. ***P < 0.001 compared with 0.25 mg/kg Coversin. §P < 0.05, and §§§P < 0.001 for 2.5 mg/kg Coversin vs. 0.025 mg/kg Coversin. +P < 0.05, and ++P < 0.01 for 0.25 mg/kg Coversin vs. 0.025 mg/kg Coversin. (**C**) Peak value of ABSA determined individually for each mouse. (**D**) C5a serum levels on day 10. Results presented in **C** and **D** were pooled from 2 independent experiments (n = 9–11 mice/group) and are shown as mean ± SEM with dots representing individual mice. Data were analyzed using 1-way ANOVA with Holm-Šídák's multiple-comparisons test. *P < 0.05, **P < 0.01, ***P < 0.001 for the comparisons indicated by dashed lines.

effect on each other's binding to OmCI (16). This unique bifunctional pharmacological activity highlights OmCI as a potentially highly effective therapeutic compound in diseases collaboratively driven by C5a and LTB_4. In recombinant form, OmCI is known as "Coversin" and is currently in a phase III clinical trial (NCT03588026) for treatment of paroxysmal nocturnal hemoglobinuria.

Although binding of Coversin to C5 and to LTB_4 is functionally independent (15, 16), binding of C5 to Coversin indirectly affects its ability to sequester LTB_4 over long periods because binding to C5 prolongs the half-life of Coversin in the murine circulation from less than 20 minutes to approximately 10 hours (13). The half-life of Coversin in the circulation of mice when not bound to C5 can be extended to 10.2 hours by PASylation, which is the in-frame N-terminal fusion of a 600–amino acid tail composed of repetitions of the tripeptide sequence Pro Ala Ser to Coversin, thus, yielding PAS-Coversin (17, 18). The extension of the half-life by PASylation is important for the clinical development of L-Coversin, a bioengineered variant of Coversin mutated at 7 amino acids to ablate binding to C5, which therefore

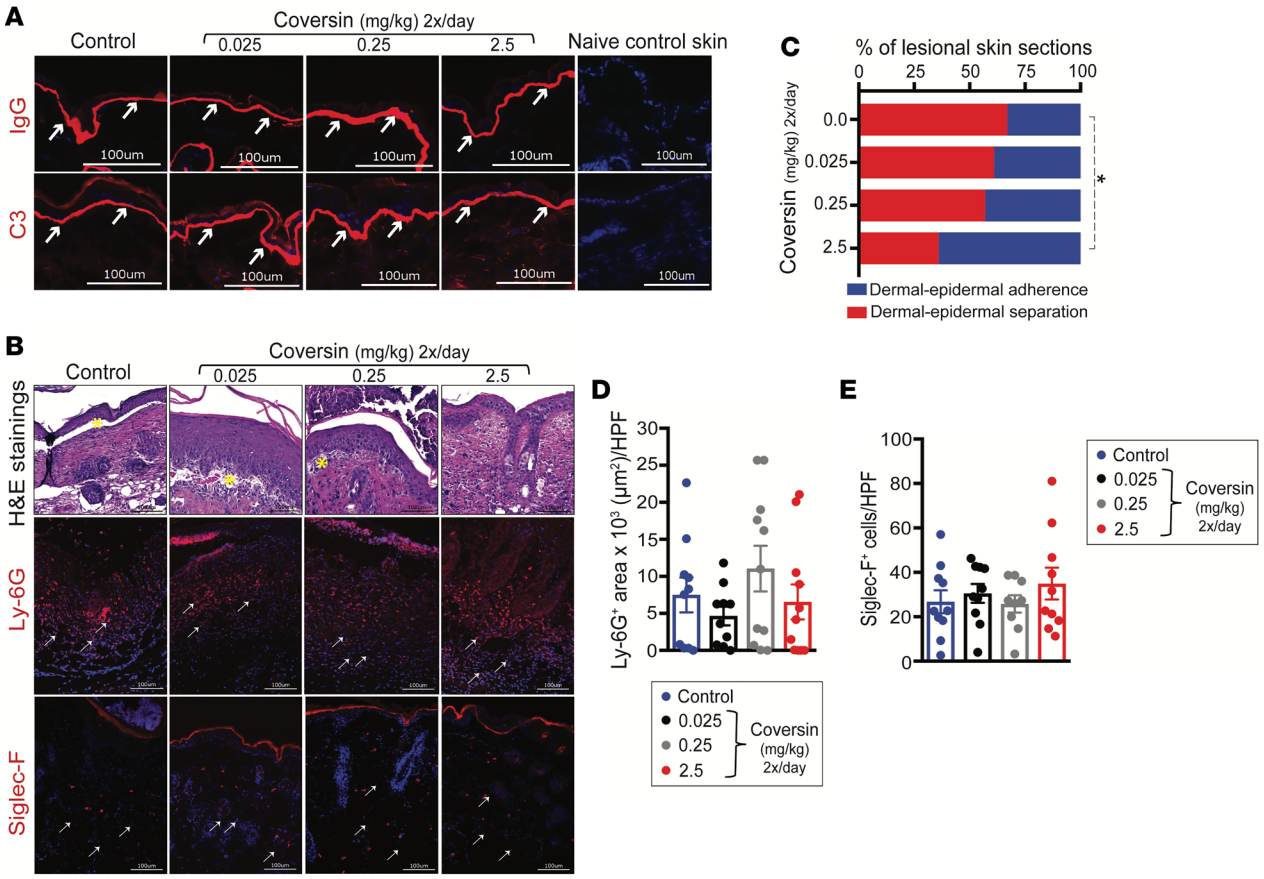

Figure 2. Effect of preventative treatment with varying doses of Coversin on skin inflammation at the histopathological level. Histopathological analysis and comparison of skin from mice treated with varying doses of Coversin in a preventative treatment regimen and harvested on day 10 of the antibody transfer BP-like EBA model. (**A**) Representative direct immunofluorescence microscopy pictures of staining for IgG (upper) and C3 (lower) in perilesional skin. The arrows indicate the linear deposition of IgG and C3, respectively, at the DEJ. (**B**) Representative pictures of H&E staining (upper) and immunofluorescence staining for Ly-6G (middle) and Siglec-F (lower). Asterisks in the upper images indicate subepidermal clefts; arrows in the middle and lower images indicate examples for Ly-6G$^+$ (neutrophils) and Siglec-F$^+$ (eosinophils) cells, respectively. (**C**) Percentage of lesional skin sections exhibiting (red) or not exhibiting (blue) subepidermal clefts. (**D**) Ly-6G$^+$ area and (**E**) number of Siglec-F$^+$ cells per high-power magnification field (HPF; original magnification, ×200). Scale bars: 100 µm. Results were pooled from 2 independent experiments and are presented as mean ± SEM with dots representing individual mice (n = 9–11 mice/group). Data in **C** were analyzed by χ^2 test followed by Fisher's exact test. *P < 0.05.

exclusively binds LTB_4. Because L-Coversin does not bind C5, its half-life in murine circulation is less than 20 minutes and, therefore, too short for therapeutic application; thus, PASylation of L-Coversin is a prerequisite for its use as a parenteral drug.

In the present study, we have examined the therapeutic potential of Coversin and PAS–L-Coversin in the antibody transfer model of BP-like EBA. We found that both compounds significantly ameliorate skin inflammation, but the therapeutic effect of Coversin is more pronounced than that of PAS–L-Coversin, suggesting that dual inhibition of C5 and LTB_4 is advantageous. We also provide further evidence that C5a and LTB_4 are functionally active in lesional skin of patients with BP. Collectively, our results highlight both Coversin and PAS–L-Coversin as potential drugs for the treatment of BP and possibly other PDs.

Results

Coversin dose dependently suppresses murine BP-like EBA. To determine the potential of dual C5 and LTB_4 inhibition as a novel therapeutic principle, we examined the effect of different doses of Coversin on the course of disease. For this purpose, 0.025, 0.25, and 2.5 mg/kg body weight Coversin were administered s.c. twice daily, starting 4 days before the first injection of anti–COL7c IgG (day –4), into C57BL6/J wild-type mice. Control mice received only vehicle (0.01 M PBS, pH 7.2). Under this regimen, Coversin dose dependently attenuated

skin inflammation throughout the time of observation (Figure 1, A–C). The results show that 0.25 mg/kg and 2.5 mg/kg Coversin were equally effective and reduced peak disease by approximately 50% (Figure 1, B and C) whereas 0.025 mg/kg Coversin only slightly attenuated disease (Figure 1, A–C).

C5a serum levels were significantly increased in mice suffering from BP-like EBA but were attenuated in mice treated with 2.5 mg/kg Coversin when determined 12 hours after the last administration of Coversin (Figure 1D). LTB_4 serum levels were not determined because it is technically not possible to distinguish free from Coversin-bound LTB_4.

By direct immunofluorescence microscopy, we excluded the possibility that the therapeutic effect of Coversin was due to compromised IgG or complement factor 3 (C3) deposition at the DEJ (Figure 2A). In those skin lesions emerging despite Coversin treatment, the frequency of dermal-epidermal cleft formation was lower at the 2.5 mg/kg dose (Figure 2, B and C), although the density of granulocytes in the dermal infiltrate was not reduced by Coversin (Figure 2, B, D, and E). As anticipated, C5aR1 was expressed on neutrophils in the dermal infiltrate (Supplemental Figure 1A; supplemental material available online with this article; https://doi.org/10.1172/jci.insight.128239DS1). The density of $C5aR1^+$ neutrophils was not altered under Coversin treatment either (Supplemental Figure 1B). Because no antibodies against murine BLT1 are commercially available, we did not have the chance to confirm the anticipated expression of BLT1 at the protein level in the inflammatory infiltrate.

PAS–L-Coversin reduces BP-like EBA but less effectively than Coversin. We examined whether PAS–L-Coversin is effective in the antibody transfer BP-like EBA mouse model. We administered 0.1, 1.0, and 10.0 mg/kg body weight PAS–L-Coversin s.c. once daily starting 4 days before the first injection of anti–COL7c IgG (day –4). To directly compare PAS–L-Coversin with Coversin, another group was treated twice daily with 2.5 mg/kg Coversin, which is the molar equivalent dose to 10.0 mg/kg PAS–L-Coversin. The control group received vehicle s.c. once daily. PAS–L-Coversin dose dependently attenuated skin inflammation throughout the entire observation time (Figure 3A). A dose of 10.0 mg/kg PAS–L-Coversin reduced disease activity by approximately 50% and reduced peak disease severity by approximately two-thirds (Figure 3, B and C). It was, however, less effective in the clinical outcome than 2.5 mg/kg Coversin (Figure 3, A–C). As expected, Coversin but not PAS–L-Coversin reduced C5a serum levels (Figure 3D).

At the histopathological level, Coversin but not PAS–L-Coversin significantly reduced the frequency of dermal-epidermal cleft formation (Figure 4, A and B); however, neither drug reduced granulocyte infiltration in lesional skin harvested on day 12 of the experiment (Figure 4, B–D, and Supplemental Figure 2). Immunofluorescence (IF) stains for IgG and C3 depositions at the DEJ on day 12 excluded the possibility that the therapeutic effects of Coversin or PAS–L-Coversin were caused by reduced deposition of IgG or C3 (results not shown).

Coversin halts ongoing BP-like EBA. To determine whether Coversin is also effective in abrogating ongoing skin inflammation, BP-like EBA was induced in wild-type mice before treatment with 0.125 or 2.5 mg/kg Coversin s.c. twice daily was initiated on day 5. Thus, 2.5 mg/kg Coversin rapidly attenuated the further progression of skin inflammation (Figure 5, A–C). The peak of disease in the 2.5 mg/kg Coversin treatment group was reduced by approximately 40% compared with the vehicle control group (Figure 5, B and C). In contrast, 0.125 mg/kg Coversin only modestly reduced disease. C5a serum levels still tended to be decreased 12 hours after the last administration of 2.5 mg/kg but not of 0.125 mg/kg Coversin (Figure 5D). A dose of 2.5 mg/kg Coversin significantly reduced dermal-epidermal cleft formation and neutrophil infiltration but not eosinophil infiltration in lesional skin (Figure 6, A–D, and Supplemental Figure 3).

LTB_4 and C5a are present in relevant quantities in BP blister fluid. The content of LTB_4 and of C5a in the blister fluid of patients with BP was assayed. Both LTB_4 and C5a were present in the blister fluid of all patients with BP included in this study. The levels of LTB_4 were in the range of 0.2 to 1.2 ng/mL with a median of 0.46 ng/mL (Figure 7A). The levels of C5a were in the range of 3.6 to 19.4 ng/mL with a median of 11 ng/mL (Figure 7B). At these concentrations, C5a and LTB_4 both induced the migration of human neutrophils in vitro (Figure 7, C and D).

IF staining revealed that both C5aR1 and BLT1 were expressed at low levels in the skin of healthy controls but were both abundant in perilesional skin of patients with BP (Figure 8, A and B, and Supplemental Figure 4, A and B). C5aR1 expression was predominantly detectable on keratinocytes (Figure 8A). BLT1, in contrast, was not detectable in the epidermis, but was abundant in the dermis. To identify the cell type(s) expressing BLT1 in the dermis, perilesional skin was first profiled for dermal infiltration of major basic protein (MBP), myeloperoxidase (MPO), and $CD68^+$ cells (Figure 8, C and D, and Supplemental Figure 4C).

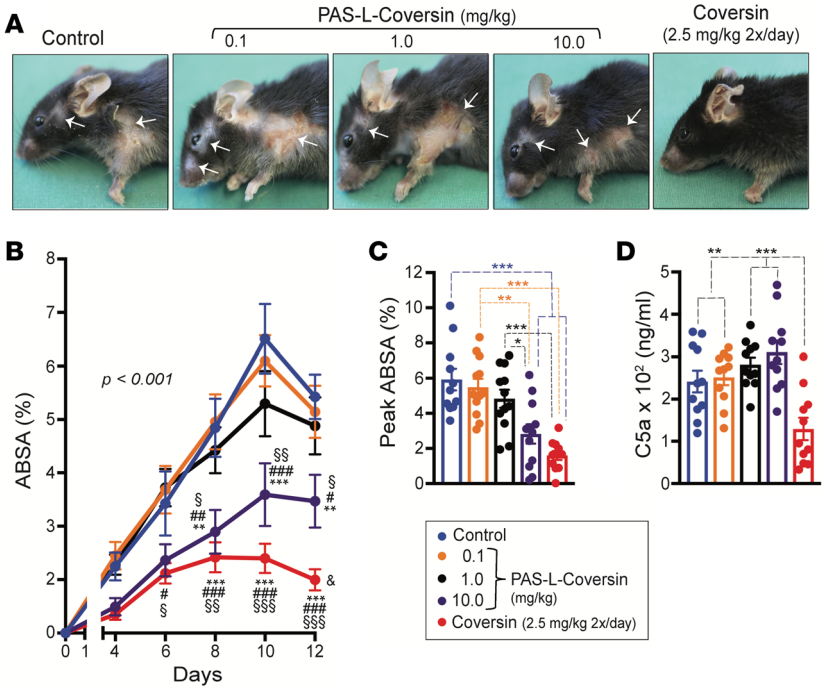

Figure 3. PAS–L-Coversin reduces skin inflammation. Effect of varying doses of PAS–L-Coversin administered once daily in comparison with Coversin (2.5 mg/kg) administered twice daily starting 4 days before the first application of anti-COL7c IgG in the antibody transfer BP-like EBA mouse model. (**A**) Representative pictures of clinical presentation on day 12. White arrows indicate BP-like EBA skin lesions. (**B**) Progression of disease determined by the percentage of the total ABSA. Results are presented as mean ± SEM and were analyzed using 2-way ANOVA with Holm-Šídák's multiple-comparisons test. $^{**}P < 0.01$, and $^{***}P < 0.001$ compared with control. $\#P < 0.05$, $\#\#P < 0.01$, and $\#\#\#P < 0.001$ compared with 0.1 mg/kg PAS–L-Coversin. $\S P < 0.05$, $\S\S P < 0.01$, and $\S\S\S P < 0.001$ compared with 1 mg/kg PAS–L-Coversin. $\&P < 0.05$ compared with 10.0 mg/kg PAS–L-Coversin. (**C**) Peak value of the ABSA and (**D**) C5a serum levels on day 12 presented as mean ± SEM with dots representing individual mice. Data were analyzed using 1-way ANOVA with Holm-Šídák's multiple-comparisons test. $^{*}P < 0.05$, $^{**}P < 0.01$, $^{***}P < 0.001$ for the comparisons indicated by dashed lines. All results shown were pooled from 2 independent experiments (n = 11–12 mice/group).

MBP is a cell marker of eosinophils, MPO of neutrophils and inflammatory monocytes, and CD68 of macrophages. This revealed that these 3 myeloid cell types are often present in perilesional BP skin and that the infiltrate is dominated in most cases by eosinophils and macrophages. Subsequent double stains for these cell markers and BLT1 in lesional BP skin uncovered that BLT1 is expressed mainly on eosinophils (Figure 8, C and E, and Supplemental Figure 4C).

Discussion

The efficacy of Coversin in suppressing inflammation in C5-driven conditions has previously been reported for thrombotic microangiopathy, polymicrobial sepsis, antiphospholipid syndrome, myasthenia gravis, and myocardial infarction, among others (19–25). In contrast, the effect of Coversin on conditions driven by LTB_4 has been investigated only in an acute, 4-hour-long mouse model of immune complex–induced lung injury, where the inhibition of both C5 and LTB_4 by Coversin contributed to the therapeutic effect (15). Here, we examined the therapeutic potential of dual inhibition of C5 and LTB_4 by Coversin and of single inhibition of LTB_4 by PAS–L-Coversin, in the antibody transfer model of BP-like EBA, a prototypical mouse model of the effector phase of PDs, depending on both C5a and LTB_4 (26). Both Coversin and PAS–L-Coversin suppressed skin inflammation in this model, but Coversin did so more effectively than PAS–L-Coversin, indicating that dual inhibition of LTB_4 and C5a synergizes in reducing skin inflammation. The result supports the concept that targeting more than 1 disease-driving pathway simultaneously is therapeutically advantageous because it may overcome pathway redundancy and counter-regulatory pathways (27–29).

Notably, Coversin not only reduced skin inflammation when administered in a preventative regimen but also potently and swiftly reversed ongoing skin inflammation, indicating that C5a and LTB_4

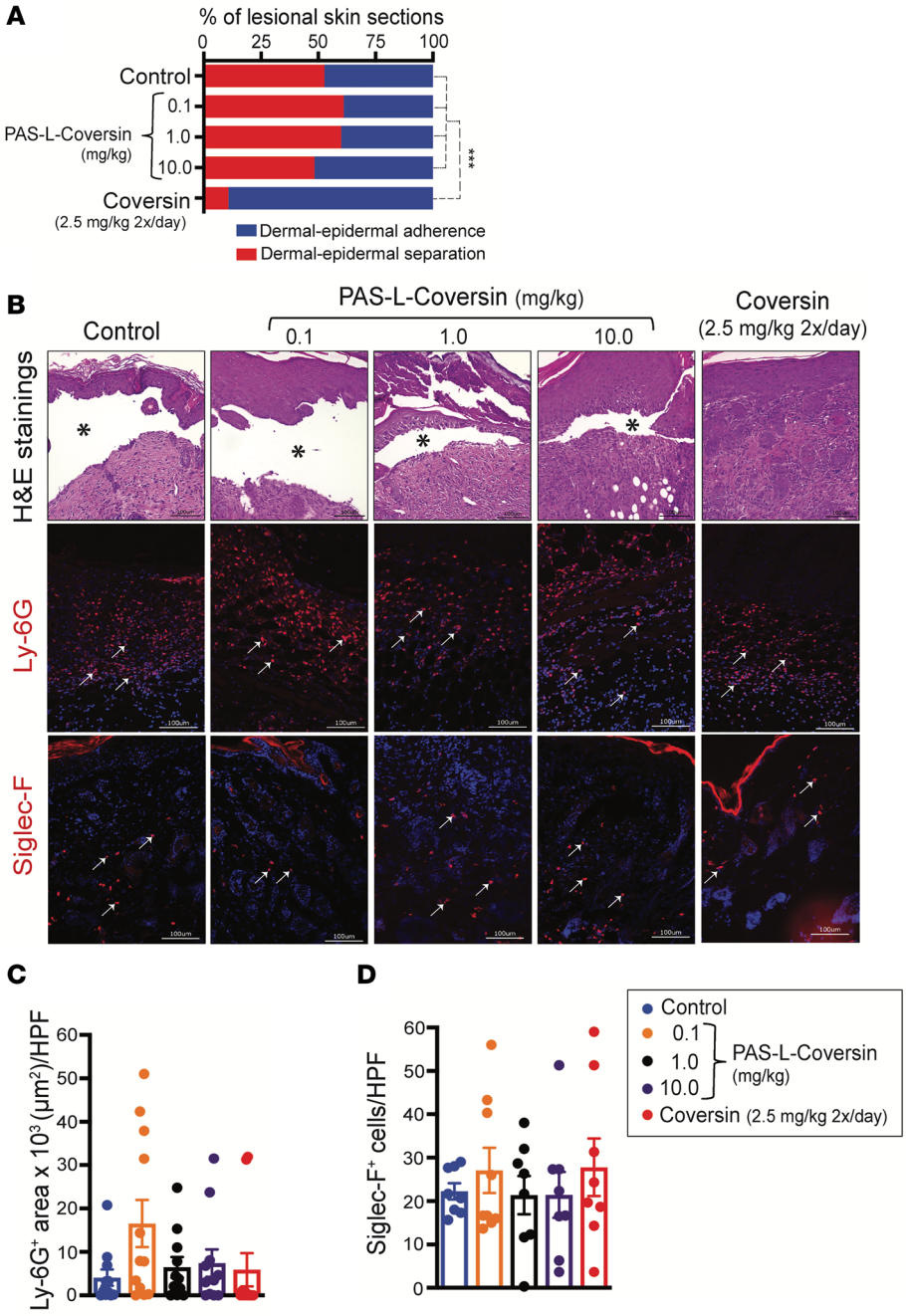

Figure 4. Effect of treatment with PAS-L-Coversin on skin inflammation at the histopathological level. Histopathological analysis and comparison of skin biopsies from mice treated with varying doses of PAS-L-Coversin or Coversin started 4 days before the first application of anti-COL7c IgG and harvested on day 12 of the antibody transfer BP-like EBA model. (**A**) Percentage of lesional skin sections exhibiting (red) or not exhibiting (blue) subepidermal clefts. (**B**) Representative pictures of H&E staining (upper) and immunofluorescence staining for Ly-6G (middle) and Siglec-F (lower). Asterisks in the upper images indicate subepidermal clefts; arrows in the middle and lower images indicate examples for Ly-6G$^+$ (neutrophils) and Siglec-F$^+$ (eosinophils) cells, respectively. (**C**) Ly-6G$^+$ area and (**D**) number of Siglec-F$^+$ cells per HPF at original magnification of ×200. Scale bars: 100 µm. Results were pooled from 2 independent experiments and are presented as mean ± SEM; dots represent individual mice (n = 8–12 mice/group). Data in **A** were analyzed by χ^2 test followed by Fisher's exact test. ***$P < 0.001$ for the comparisons indicated by dashed lines.

permanently contribute to the progression of skin inflammation and do not become dispensable in later stages of the pathogenic process because of elaboration of immunopathogenic pathways. An ongoing requirement for complement activation products and proinflammatory eicosanoids to sustain disease has previously been suggested for other antibody-driven disorders (30, 31).

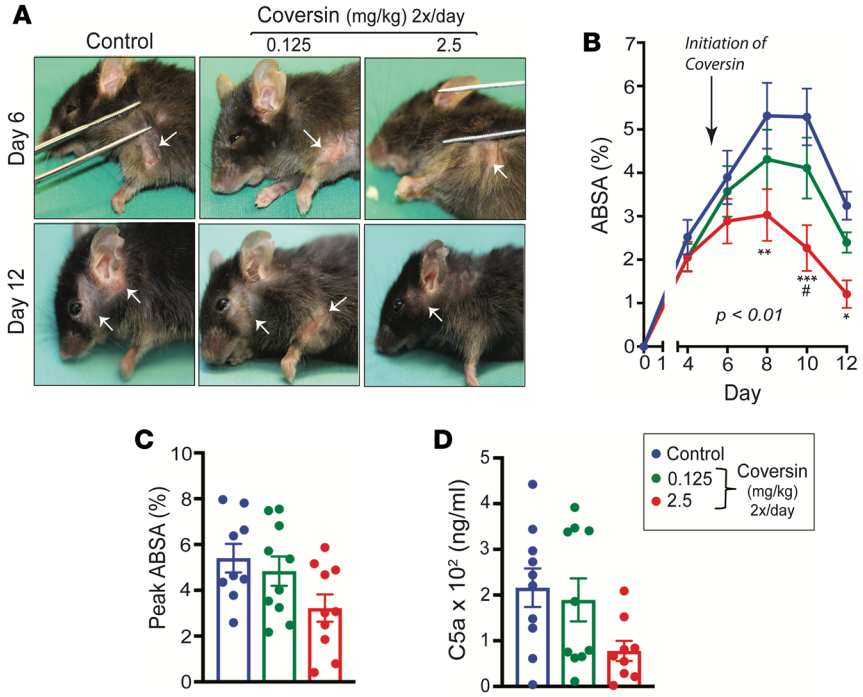

Figure 5. Coversin ablates the progression of ongoing skin inflammation. Therapeutic effect of treatment with Coversin initiated on day 5. (**A**) Representative clinical presentation on day 6, one day after the initiation of Coversin therapy, and at the end of the experiment on day 12. White arrows indicate BP-like EBA skin lesions. (**B**) Progression of disease determined by the percentage of the total ABSA as mean ± SEM. Data were analyzed by 2-way ANOVA with Holm-Šídák's multiple-comparisons test. $*P < 0.05$, $**P < 0.01$, and $***P < 0.001$ compared with control. $\#P < 0.05$ compared with 0.125 mg/kg Coversin. (**C**) Peak value of the ABSA determined for each mouse individually and (**D**) C5a serum levels (ng/mL) on day 12 presented as mean ± SEM with dots representing individual mice (n = 9–11 mice/group). In **D**, data were analyzed using 1-way ANOVA with Holm-Šídák's multiple-comparisons test. All results shown were pooled from 2 independent experiments.

The source of C5a and LTB_4 as well as their functional and spatiotemporal relationship in the pathogenesis of PDs is still unresolved. C5a generation may be initiated in the skin upon C3 deposition at the DEJ by the complement pathway tick-over mechanism, and the LTB_4 produced is most likely predominantly derived from neutrophils, which release copious amounts of LTB_4 upon activation by C5a or immune complexes (32).

C5a and LTB_4 have previously been highlighted as indispensable for the emergence of skin inflammation in the BP-like EBA mouse model (4, 26). Both mediators can, in general, act as chemoattractants and activators of neutrophils. In the latter function, they induce, e.g., the release of radical oxygen species and proteases from neutrophils (33–35). Both recruitment and activation of neutrophils in the skin are essential for the development of skin lesions and, presumably, mutually modulate each other in the BP-like EBA mouse model (36, 37). As a corollary, the disruption of recruitment and activation of neutrophils both can potentially contribute to the therapeutic effects of Coversin and PAS–L-Coversin observed in the BP-like EBA model. Accordingly, Coversin and PAS–L-Coversin reduced the percentage of the total body surface area affected by skin lesions, which is likely, at least partially, a result of inhibition of neutrophil recruitment into the skin and is in line with the previously reported complete resistance of *Alox5*$^{-/-}$ and *Ltb4r1*$^{-/-}$ mice to neutrophil recruitment into the skin in this model. Additionally, Coversin but not PAS–L-Coversin significantly reduced dermal-epidermal cleft formation in lesional skin, which is likely the result of decreased neutrophil activation in the skin. The reason for this difference between Coversin and PAS–L-Coversin may be possible differences in the pharmacokinetics of PAS–L-Coversin and Coversin as well as differences in the roles of C5a and LTB_4 as activators of neutrophils in the skin. Thus, our results suggest that C5a may be more important than LTB_4 for the activation of neutrophils in the skin.

Examining blister fluid of patients with BP, we demonstrated that C5 is proteolyzed to C5a in BP skin

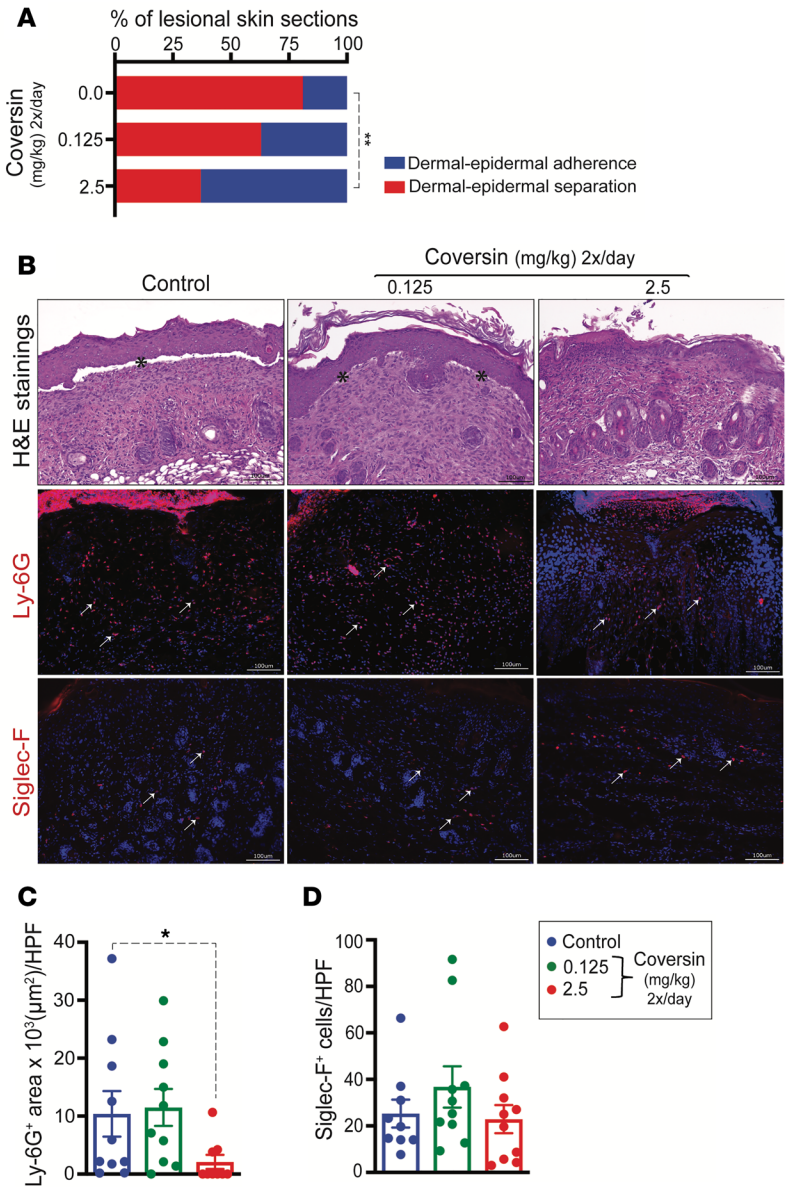

Figure 6. Effect of Coversin treatment initiated in ongoing BP-like EBA at the histopathological level. Histopathological analysis and comparison of skin biopsies from mice treated with varying doses of Coversin in a preventative treatment regimen and harvested on day 12 of the antibody transfer BP-like EBA model. (**A**) Percentage of lesional skin sections exhibiting (red) or not exhibiting (blue) subepidermal clefts. (**B**) Representative pictures of H&E staining (upper) and IF staining for Ly-6G (middle) and Siglec-F (lower). Asterisks in the upper images indicate subepidermal clefts; arrows in the middle and lower images indicate examples for Ly-6G$^+$ (neutrophils) and Siglec-F$^+$ (eosinophils) cells, respectively. (**C**) Ly-6G$^+$ area and (**D**) number of Siglec-F$^+$ cells per HPF at original magnification of ×200. Scale bars: 100 µm. Results were pooled from 2 independent experiments and are presented as mean ± SEM; dots represent individual mice (n = 9–10 mice/group). Data in **A** were analyzed by χ^2 test followed by Fisher's exact test; $^{**}P < 0.01$ for the comparisons indicated by dashed lines. Data in **C** were analyzed by Kruskal-Wallis test using Dunn's multiple-comparisons test. $^*P < 0.05$ for the comparisons indicated by dashed lines.

lesions, which extends previous studies showing that C5 is deposited at the DEJ in BP (11). Furthermore, we confirmed previous reports that blister fluid is rich in LTB_4 (9, 10). Both C5a and LTB_4 are most likely generated in the dermis. Accordingly, the levels of both mediators reached in the dermis are presumably significantly higher than in the blister fluid. Collectively, our results support the notion that both C5a and LTB_4 may play a role as chemoattractants and activators of granulocytes in the skin in bullous diseases.

Our IF staining for BLT1 in lesional skin of patients with BP detected BLT1 predominantly on eosinophils infiltrating the dermis. Expression of C5aR1 was low in the dermis but marked on keratinocytes.

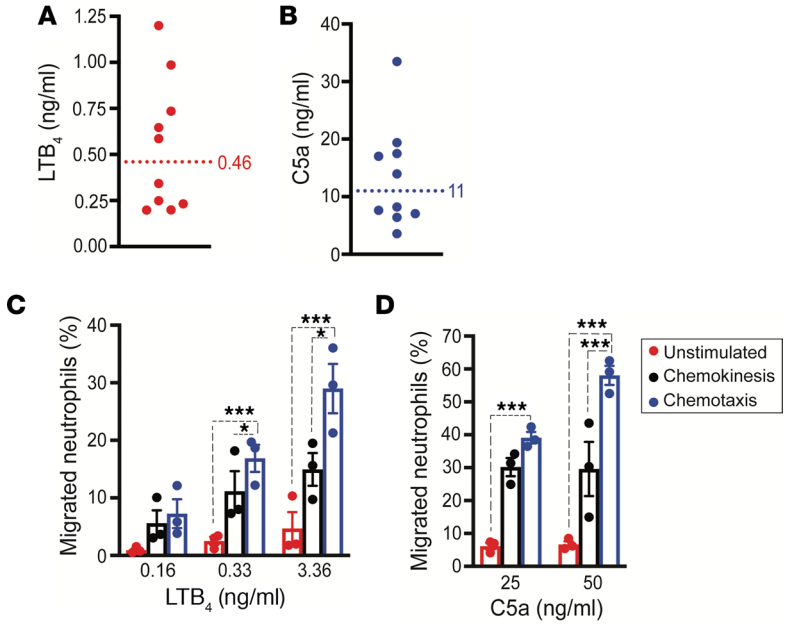

Figure 7. C5a and LTB_4 are present in blister fluid of patients with BP in functionally relevant concentrations. Levels of (**A**) LTB_4 and (**B**) C5a (ng/mL) in skin blister fluid from 10 patients with BP. Each dot represents 1 patient. The colored, dotted lines indicate the mean. Chemokinesis and chemotaxis of human neutrophils in response to varying concentrations of (**C**) LTB_4 and (**D**) C5a. Results shown are compiled from 3 independent experiments and are presented as mean ± SEM of migrated cells (percentage) with each dot representing 1 experiment. Data in **C** and **D** were analyzed with 1-way ANOVA with Holm-Šídák's multiple-comparisons test. $^*P < 0.05$, $^{***}P < 0.001$ for the comparisons indicated by dashed lines.

The high expression of C5aR1 on keratinocytes specifically in lesional skin suggests that pathogenic stimuli upregulate C5aR1 expression. Knowledge on the role of C5aR1 on keratinocytes is scarce. A previous study reported that C5aR1 mRNA is induced in keratinocytes under different inflammatory conditions (38), but the functional significance of C5aR1 on keratinocytes has not been addressed.

The findings of this study provide good reason to examine the therapeutic potential of Coversin and PAS–L-Coversin in patients with PD. The introduction of either into therapy has the potential to substantially improve treatment of PD from untargeted, general immunosuppression to a pathogenic pathway–specific, targeted strategy afflicted with fewer side effects than current treatments. Consequently, based on the preclinical data presented here, a phase II clinical trial of the therapeutic potential of Coversin in patients with BP has been initiated (EudraCT number 20178-002836-18).

Methods

Mice. C57BL/6J wild-type mice were purchased from Janvier Labs. Animals were bred and housed in a 12-hour light/12-hour dark cycle at the animal facility of the University of Lübeck. All experiments were approved by the Schleswig-Holstein state government and performed on 8- to 12-week-old age- and sex-matched mice by certified personnel.

Induction and scoring of antibody transfer BP-like EBA. Antibody transfer BP-like EBA was induced, as previously described (4). Briefly, New Zealand rabbits were immunized against 3 epitopes of type VII collagen, and IgG directed against the epitope C (anti-COL7c) was affinity purified, as previously described. The purified anti–COL7c IgG antibody was assessed for its reactivity to murine Col7 by indirect IF microscopy performed on murine tail skin sections, as previously described (4). We injected 50 μg anti-COL7c s.c. into the neck, right foreleg, and left hind leg on days 0, 2, and 4 of the experiment, respectively. The percentage of the total body surface presenting with erythema, blisters, erosions, crusts, or alopecia was determined at the time points indicated.

Treatment with Coversin and PAS–L-Coversin. Daily treatment with Coversin (0.025, 0.25, and 2.5 mg/kg body weight twice daily) or PAS–L-Coversin (0.1, 1.0, and 10.0 mg/kg body weight once daily) was initiated 4 days before the induction of BP-like EBA or on day 5 after the induction, as indicated. The control

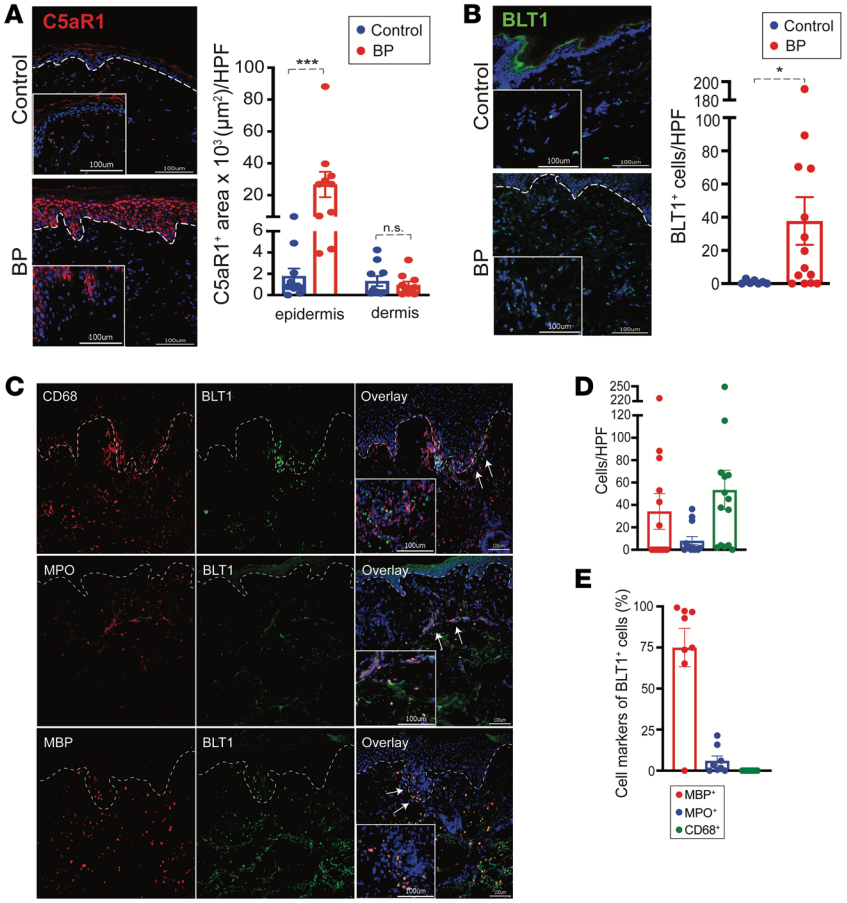

Figure 8. C5aR1 and BLT1 are abundantly expressed in perilesional skin of patients with BP. Analysis of C5aR1 and BLT1 expression in perilesional skin of patients with BP. Representative IF staining pictures of (**A**) C5aR1 and (**B**) BLT1 expression in the skin of healthy controls (n = 7) and in perilesional skin of patients with BP (n = 10–14) in an acute flare and the quantification of their expression as C5aR1$^+$ area/μm^2/HPF in the epidermis and dermis and BLT1$^+$ cells/HPF in the dermis, respectively. (**C**) Representative IF staining pictures for the expression of the cell marker proteins CD68 (macrophages), MPO (neutrophils), and MBP (eosinophils) in perilesional skin of patients with BP and their coexpression with BLT1. The pictures were taken at original magnification of ×200; inlays were digitally enlarged from the original pictures by 3-fold. (**D**) Quantification of MBP$^+$, MPO$^+$, and CD68$^+$ cells' infiltration in perilesional skin determined by IF staining (n = 15). (**E**) Percentage of BLT1$^+$ cells among MBP$^+$, MPO$^+$, and CD68$^+$ cells in perilesional skin (n = 8). Results are presented as mean ± SEM. Data in **A** and **B** were analyzed using Mann-Whitney U test. *P < 0.05, ***P < 0.001. Scale bars: 100 μm.

group received s.c. the vehicle only, 100 μL 0.01 M PBS, pH 7.2.

Histopathology. Biopsies, taken from perilesional skin, were fixed in 4% Histofix solution (Carl Roth), paraffin embedded, and cut into 6-μm sections before H&E staining. The frequency of dermal-epidermal separation (DES) at the microscopic level in these sections was determined by averaging the number of sections showing DES in three ×100-magnified histopathological images per mouse.

IgG and C3 deposition. To assess IgG and C3 deposition in the skin, direct IF stains were performed, as previously described (4), with some minor modifications. Briefly, acetone-fixed, 6-μm skin cryosections were washed with 0.01 M PBS, pH 7.2, and stained for 1 hour at room temperature with Alexa Fluor 594 AffiniPure donkey anti–rabbit IgG (Jackson ImmunoResearch Laboratories, 711-585-152) or purified rat anti–mouse complement C3 IgG (CEDARLANE, clone 10C7). To stain for C3, slides were washed and additionally incubated with Alexa Fluor 594 AffiniPure goat anti–rat IgG (Jackson ImmunoResearch Laboratories, 112-585-003) for 1 hour at room temperature. After being washed, all slides were mounted with DAPI fluoromount G (SouthernBiotech). Images were taken under ×200 magnification on a BZ-9000E series microscope (Keyence GmbH) and subsequently digitally magnified ×3 using the BZ II Analyzer (Keyence GmbH).

Quantification of neutrophil and eosinophil infiltration. Biopsies of perilesional skin were stained for

the neutrophil marker Ly-6G and the eosinophil marker Siglec-F, as previously described, with minor modifications (4). Briefly, for Ly-6G staining, 6-μm paraffin sections were deparaffinized, treated with pepsin digest-ALL 3 solution (Thermo Fisher Scientific) for 10 minutes at room temperature, washed 3 times with 0.01 M TBS pH 7.6, and blocked with 5% normal goat serum (NGS) for 1 hour before rat anti–mouse Ly-6G antibody (BioLegend, clone 1A8) was added in 5% (*v*/*v*) NGS for overnight incubation at 4°C. For Siglec-F staining, 6-μm cryosections were fixed with cold acetone for 10 minutes at –20°C. After 3 washes with 0.01 M PBS, pH 7.2, slides were blocked with 5% (*v*/*v*) NGS for 1 hour and incubated with rat anti–mouse Siglec-F (BD Biosciences, clone E50-2440) at 4°C overnight. After overnight incubation, slides for both stains were first washed with their respective washing buffer before incubation with Alexa Fluor 594 AffiniPure goat anti–rat IgG (Jackson ImmunoResearch Laboratories, 112-585-003) for 1 hour at room temperature. Afterward, slides were washed again and mounted with DAPI fluoromount G (SouthernBiotech). Images were acquired on a BZ-9000E series microscope (Keyence GmbH) and analyzed using a BZ II Analyzer (Keyence GmbH). Neutrophil and eosinophil infiltration in the skin was quantified by determining the percentage of the Ly-6G$^+$ area and the number of Siglec-F$^+$ cells, respectively, averaged from three ×200-magnification fields for each mouse.

Immunohistochemistry for C5aR1 and BLT1 in human skin. Biopsies were taken from lesional skin of patients with BP in an acute flare and from skin of healthy donors. Subjects were recruited at the University of Lübeck (Lübeck, Germany). To detect C5aR1, paraffin sections were stained using rabbit anti–C5aR1 antibody (Thermo Fisher Scientific, PA5-32683) and Alexa Fluor 594 AffiniPure donkey anti–rabbit IgG (Jackson ImmunoResearch Laboratories, 711-585-152) as a secondary antibody. BLT1 was detected by adding FITC-conjugated mouse anti–human BLT1 IgG (Bio-Rad, clone 202/7B1) using respective cryosections. To identify the cellular site of expression, costaining was performed with rabbit anti–human MPO for neutrophils (DAKO, A0398), mouse anti–human MBP for eosinophils (Bio-Rad, clone BMK-13), or mouse anti–human CD68 for macrophages (Thermo Fisher Scientific, clone KP1). Alexa Fluor 594 AffiniPure donkey anti–rabbit IgG (Jackson ImmunoResearch Laboratories, 711-585-152) or anti–mouse IgG (Jackson ImmunoResearch Laboratories, 715-585-151) was applied as a secondary antibody. All stains were visualized, photographed, and evaluated using the BZ-9000E series microscope (Keyence GmbH). The staining protocols are described in more detail in Supplemental Methods. To generate larger insets, original ×200-magnification images were digitally magnified ×3 using the BZ II Analyzer software (Keyence GmbH).

LTB_4 and C5a quantification. LTB_4 and C5a were quantified using the LTB_4 parameter assay and the mouse C5a DuoSet ELISA kit (R&D Systems) or the Complement C5a Human ELISA Kit (Abcam), according to the manufacturers' instructions.

Collection of blister fluid. Blister fluid was collected from patients with BP, suffering from the first flare of BP, before the initiation of treatment.

Chemotaxis assays. Chemotaxis of human neutrophils, freshly isolated from healthy volunteers (from University of Lübeck, Lübeck, Germany) using the MACSxpress Whole Blood Neutrophil Isolation Kit (Miltenyi Biotec) and resuspended to a density of 2×10^6 neutrophils/mL in phenol red–free RPMI-1640 (MilliporeSigma) with 10% heat-inactivated fetal bovine serum (Thermo Fisher Scientific), toward different concentrations of LTB_4 (Cayman Chemical) or human recombinant C5a (PeproTech) was assessed in nonbinding 96-well plates (Corning). We placed 5×10^4 neutrophils per well on top of the bottom wells of the plates on a 3-μm polycarbonate membrane (Costar Nucleopore GmbH). For chemokinesis control, LTB_4 or C5a was added to the neutrophils on top of the membrane instead of to the bottom wells. The plate was incubated for 1 hour at 37°C and 5% CO_2. Afterward, the chamber was disassembled, and migrated neutrophils were lysed by addition of 50 μL of 0.1% (*w*/*v*) hexadecyltrimethylammonium bromide solution (MilliporeSigma) for 1 hour at 37°C and 5% CO_2. The number of migrated neutrophils was determined based on their endogenous MPO activity via addition of 50 μL of 3,3′,5,5′-tetramethylbenzidine (Thermo Fisher Scientific) substrate to the migrated cells. To stop the reaction, 50 μL of 25% (*w*/*v*) sulfuric acid (Carl Roth) was added to the cells, and the optical density was measured on an InfiniteM200Pro plate reader (Tecan). To calculate the percentage of migrated neutrophils, a standard curve was generated. The original stock of isolated cells was diluted in 7 serial 2-fold dilutions and analyzed for endogenous activity of MPO similarly to the aforementioned procedure.

Statistics. All data are presented as mean ± SEM. Clinical scores and cell migrations in chemotaxis assays were compared by 2-way ANOVA with Holm-Šídák's multiple-comparisons test. Cutaneous cell

infiltrations were analyzed by Mann-Whitney *U* test or Kruskal-Wallis test with Dunn's post hoc test, when more than 2 groups were compared. ELISA results were analyzed by 2-tailed *t* test or 1-way ANOVA with Holm-Šídák's multiple-comparisons test for the comparison of more than 2 groups. The frequency of DES was assessed by χ^2 test followed by Fisher's exact test. *P* value less than 0.05 was considered statistically significant throughout the study.

All calculations were performed using GraphPad Prism 8.0 (San Diego, CA, USA).

Study approval. All mouse experiments were approved in advance by the state government of Schleswig-Holstein (Kiel, Schleswig-Holstein, Germany). All investigations involving human tissues were approved by the local institutional ethics committee of the University of Lübeck, and all participants provided written informed consent to the study.

Author contributions

CDS and MAN planned the study. TS, MAN, and CDS interpreted the results and wrote the paper. CDS also supervised the work. TS, S Murthy, CA, MS, MMH, CMH, FM, and S Mousavi conducted the experiments and analyzed the results. ES collected and provided patient specimens and edited the manuscript. DZ interpreted the results and edited the manuscript.

Acknowledgments

This research was supported by DFG funding (Sa1960/5-1) for the Clinical Research Unit 303 *Pemphigoid Diseases – Molecular Pathways and their Therapeutic Potential* and the Excellence Cluster 2167 *Precision Medicine in Chronic Inflammation*.

Address correspondence to: Christian D. Sadik, University of Lübeck, Ratzeburger Allee 160, 23538 Lübeck, Germany. Phone: 49.451.50041691; Email: christian.sadik@uksh.de.

1. Schmidt E, Zillikens D. Pemphigoid diseases. *Lancet*. 2013;381(9863):320–332.
2. Kibsgaard L, Rasmussen M, Lamberg A, Deleuran M, Olesen AB, Vestergaard C. Increased frequency of multiple sclerosis among patients with bullous pemphigoid: a population-based cohort study on comorbidities anchored around the diagnosis of bullous pemphigoid. *Br J Dermatol*. 2017;176(6):1486–1491.
3. Kridin K, Schwartz N, Cohen AD, Zelber-Sagi S. Mortality in bullous pemphigoid: a systematic review and meta-analysis of standardized mortality ratios. *J Dermatol*. 2018;45(9):1094–1100.
4. Sezin T, et al. The leukotriene B_4 and its receptor BLT1 act as critical drivers of neutrophil recruitment in murine bullous pemphigoid-like epidermolysis bullosa acquisita. *J Invest Dermatol*. 2017;137(5):1104–1113.
5. Mihai S, et al. Specific Inhibition of complement activation significantly ameliorates autoimmune blistering disease in mice. *Front Immunol*. 2018;9:535.
6. Karsten CM, et al. Anti-inflammatory activity of IgG1 mediated by Fc galactosylation and association of FcγRIIB and dectin-1. *Nat Med*. 2012;18(9):1401–1406.
7. Sitaru C, et al. Induction of dermal-epidermal separation in mice by passive transfer of antibodies specific to type VII collagen. *J Clin Invest*. 2005;115(4):870–878.
8. Karsten CM, et al. Tissue destruction in bullous pemphigoid can be complement independent and may be mitigated by C5aR2. *Front Immunol*. 2018;9:488.
9. Grando SA, Glukhenky BT, Drannik GN, Epshtein EV, Kostromin AP, Korostash TA. Mediators of inflammation in blister fluids from patients with pemphigus vulgaris and bullous pemphigoid. *Arch Dermatol*. 1989;125(7):925–930.
10. Kawana S, Ueno A, Nishiyama S. Increased levels of immunoreactive leukotriene B4 in blister fluids of bullous pemphigoid patients and effects of a selective 5-lipoxygenase inhibitor on experimental skin lesions. *Acta Derm Venereol*. 1990;70(4):281–285.
11. Provost TT, Tomasi TB Jr. Evidence for complement activation via the alternate pathway in skin diseases, I. Herpes gestationis, systemic lupus erythematosus, and bullous pemphigoid. *J Clin Invest*. 1973;52(7):1779–1787.
12. Nunn MA, et al. Complement inhibitor of C5 activation from the soft tick Ornithodoros moubata. *J Immunol*. 2005;174(4):2084–2091.
13. Hepburn NJ, et al. In vivo characterization and therapeutic efficacy of a C5-specific inhibitor from the soft tick Ornithodoros moubata. *J Biol Chem*. 2007;282(11):8292–8299.
14. Barratt-Due A, et al. Ornithodoros moubata complement inhibitor is an equally effective C5 inhibitor in pigs and humans. *J Immunol*. 2011;187(9):4913–4919.
15. Roversi P, et al. Bifunctional lipocalin ameliorates murine immune complex-induced acute lung injury. *J Biol Chem*. 2013;288(26):18789–18802.
16. Jore MM, et al. Structural basis for therapeutic inhibition of complement C5. *Nat Struct Mol Biol*. 2016;23(5):378–386.
17. Gebauer M, Skerra A. Prospects of PASylation® for the design of protein and peptide therapeutics with extended half-life and enhanced action. *Bioorg Med Chem*. 2018;26(10):2882–2887.
18. Kuhn N, Schmidt CQ, Schlapschy M, Skerra A. PASylated Coversin, a C5-specific complement inhibitor with extended pharmacokinetics, shows enhanced anti-hemolytic activity in vitro. *Bioconjug Chem*. 2016;27(10):2359–2371.

19. Goodship THJ, et al. Use of the complement inhibitor Coversin to treat HSCT-associated TMA. *Blood Adv*. 2017;1(16):1254–1258.
20. Romay-Penabad Z, et al. Complement C5-inhibitor rEV576 (coversin) ameliorates in-vivo effects of antiphospholipid antibodies. *Lupus*. 2014;23(12):1324–1326.
21. Skjeflo EW, et al. Combined inhibition of complement and CD14 improved outcome in porcine polymicrobial sepsis. *Crit Care*. 2015;19:415.
22. Huber-Lang M, et al. Double blockade of CD14 and complement C5 abolishes the cytokine storm and improves morbidity and survival in polymicrobial sepsis in mice. *J Immunol*. 2014;192(11):5324–5331.
23. Barratt-Due A, et al. Combined inhibition of complement C5 and CD14 markedly attenuates inflammation, thrombogenicity, and hemodynamic changes in porcine sepsis. *J Immunol*. 2013;191(2):819–827.
24. Soltys J, et al. Novel complement inhibitor limits severity of experimentally myasthenia gravis. *Ann Neurol*. 2009;65(1):67–75.
25. Pischke SE, et al. Complement factor 5 blockade reduces porcine myocardial infarction size and improves immediate cardiac function. *Basic Res Cardiol*. 2017;112(3):20.
26. Sadik CD, Miyabe Y, Sezin T, Luster AD. The critical role of C5a as an initiator of neutrophil-mediated autoimmune inflammation of the joint and skin. *Semin Immunol*. 2018;37:21–29.
27. Lehár J, et al. Synergistic drug combinations tend to improve therapeutically relevant selectivity. *Nat Biotechnol*. 2009;27(7):659–666.
28. Keith CT, Borisy AA, Stockwell BR. Multicomponent therapeutics for networked systems. *Nat Rev Drug Discov*. 2005;4(1):71–78.
29. Hopkins AL. Network pharmacology: the next paradigm in drug discovery. *Nat Chem Biol*. 2008;4(11):682–690.
30. Sadik CD, Luster AD. Lipid-cytokine-chemokine cascades orchestrate leukocyte recruitment in inflammation. *J Leukoc Biol*. 2012;91(2):207–215.
31. Sadik CD, Kim ND, Luster AD. Neutrophils cascading their way to inflammation. *Trends Immunol*. 2011;32(10):452–460.
32. Sadik CD, Kim ND, Iwakura Y, Luster AD. Neutrophils orchestrate their own recruitment in murine arthritis through C5aR and FcγR signaling. *Proc Natl Acad Sci USA*. 2012;109(46):E3177–E3185.
33. DiScipio RG, Schraufstatter IU, Sikora L, Zuraw BL, Sriramarao P. C5a mediates secretion and activation of matrix metalloproteinase 9 from human eosinophils and neutrophils. *Int Immunopharmacol*. 2006;6(7):1109–1118.
34. Tennenberg SD, Fey DE, Lieser MJ. Oxidative priming of neutrophils by interferon-gamma. *J Leukoc Biol*. 1993;53(3):301–308.
35. Suda T, et al. Dapsone suppresses human neutrophil superoxide production and elastase release in a calcium-dependent manner. Br J Dermatol. 2005;152(5):887–895.
36. Shimanovich I, et al. Granulocyte-derived elastase and gelatinase B are required for dermal-epidermal separation induced by autoantibodies from patients with epidermolysis bullosa acquisita and bullous pemphigoid. *J Pathol*. 2004;204(5):519–527.
37. Chiriac MT, Roesler J, Sindrilaru A, Scharffetter-Kochanek K, Zillikens D, Sitaru C. NADPH oxidase is required for neutrophil-dependent autoantibody-induced tissue damage. *J Pathol*. 2007;212(1):56–65.
38. Fayyazi A, et al. C5a receptor and interleukin-6 are expressed in tissue macrophages and stimulated keratinocytes but not in pulmonary and intestinal epithelial cells. *Am J Pathol*. 1999;154(2):495–501.